JMEPEG (1996) 5:117-123 

# Application of a Time-Dependent Constitutive Model to Rheocast Systems

*O.J. Ilegbusi*

**A mathematical model has been developed to describe the velocity field in an agitated Al-5Cu alloy in which $B_4C$ particles were suspended at different loading rates of up to 40%. The material system was agitated by means of an electromagnetic rotary stirrer. The non-Newtonian behavior of the melt/solid slurry was allowed for using two models: the steady-state model of Joly and Flemings and the model of Brown, which takes account of time-dependent behavior. Calculations have shown that the two models behave similarly at high shear rates. In addition, if agitation was discontinued, very little time was required for the velocity (and hence the fluidity) of the slurry to decay.**

**Keywords**

mathematical model, non-Newtonian flow, rheocasting, semisolid slurry, time-dependent constitutive model

## 1. Introduction

SINCE its invention by Flemings and Mehrabian (Ref 1) some 22 years ago, rheocasting has become a potentially attractive means of producing parts from segregation-prone alloys and of controlling microstructure in general. Any discussion of the production of rheocast materials must observe the basic principle that the melt/solid slurries to be handled are shear thinning, which means they become fluid when subjected to sufficiently high levels of shear. In the pioneering work of characterizing the rheological properties of these systems, Fleming's coworkers (Ref 2, 3) were able to develop constitutive relationships that enabled us to quantify the types of shear rates that are necessary to achieve conditions appropriate for rheocasting systems.

Optimal design of rheocasting equipment requires modeling the whole process, including heat transfer, fluid flow, and solidification. Furthermore, for practical reasons, in many applications it is helpful to provide the necessary agitation through the use of electromagnetic forces, which requires incorporating the concepts of magnetohydrodynamic (MHD) phenomena.

The initial work carried out in this field (Ref 4-6) has concentrated on predicting the velocity fields in melt/solid slurries, agitated by either mechanical or electromagnetic means. In the latter case, both rotary stirring and agitation provided by an axial field were considered. The work was subsequently extended to incorporate the elements of heat transfer and solidification (Ref 7).

This research was helpful, in that it provided the quantitative underpinning of the basic theory that system flowability depended on both the solid fraction and the shear rate and that maintaining high shear rates was necessary in order to have a relatively fluid system, especially at high solid fraction rates. These earlier studies developed a methodology of addressing problems of this type that can be readily extended to representing real casting applications.

A critical point in all these modeling efforts is that actual predictions will have to depend on the appropriateness of the constitutive models employed for representing the relationship between shear and strain, especially since these relationships, far from being universal, are dependent on the particular system employed. Until recently, data on these systems have been scarce; furthermore, the description of the rheology failed to address the issues of inhomogeneity and time dependence. As a practical matter, both of these phenomena could significantly affect the performance of real rheocasting units. Inhomogeneity and segregation of the solid phase may adversely affect system performance. An understanding of transient behavior is, of course, crucial to addressing casting applications where the melt is not actually being stirred upon entering the mold. In simple terms, it would be essential to know how long the melt would retain its fluidity once agitation has been discontinued or once it leaves the region where external agitation is being imposed on the system.

The purpose of this work is to review our earlier efforts in modeling electromagnetically stirred rheocasting systems and then to extend these calculations by allowing for the time dependence of these systems through the incorporation of constitutive relationships recently developed by Brown (Ref 8). Section 2 presents a formulation of the problem and describes the numerical method employed for the solution of the differential equations. The computed results are presented in Section 3 and discussed in Section 4.

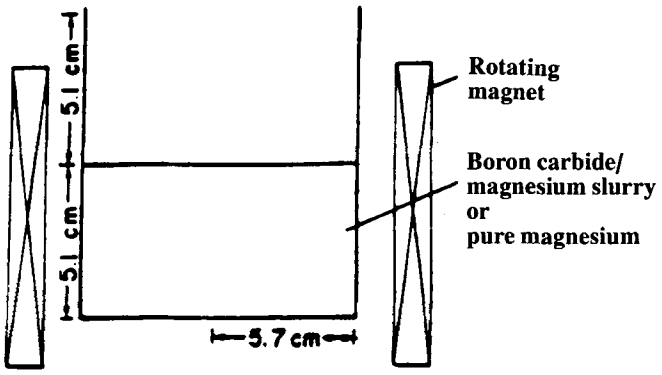


**Fig. 1** Schematic of system considered

**O.J. Ilegbusi,** Department of Mechanical, Industrial and Manufacturing Engineering, Northeastern University, Boston, MA 02115, USA.

## 2. Formulation

Consider a cylindrical vessel (Fig. 1) that contains an initially molten alloy in which inert solid particles are suspended. The material chosen for the calculations was an Al-5Cu alloy in which boron carbide particles were suspended.

This melt is being agitated by a rotating electromagnetic field of the type described in Ref 6. There are two main assumptions:

- The system is axisymmetric.
- Flow in the melt can be described by the two-dimensional Navier-Stoke's equations, with an appropriate shear-thinning model to represent the effective viscosity of the melt. Thus, the melt viscosity will depend on the solid fraction and on the shear rate. Since the shear rate is both direction and position dependent, this relationship will be quite complex.

Within the framework of these assumptions, the governing equations may be put in the form:

*Mass conservation:*

$$\frac{\partial w}{\partial z} + \frac{1}{r}\frac{\partial rv}{\partial r} = 0 \qquad \text{(Eq 1)}$$

*Axial momentum:*

$$\frac{\partial \rho w}{\partial t} + \nabla \cdot (\rho \mathbf{U} w) = -\frac{\partial p}{\partial z} - (\nabla \cdot \tau)_z + F_z \qquad \text{(Eq 2)}$$

*Radial momentum:*

$$\frac{\partial \rho v}{\partial t} + \nabla \cdot (\rho \mathbf{U} v) = -\frac{\partial p}{\partial r} - (\nabla \cdot \tau)_r + F_r \qquad \text{(Eq 3)}$$

*Azimuthal momentum:*

$$\frac{\partial \rho u}{\partial t} + \nabla \cdot (\rho \mathbf{U} u) = -(\nabla \cdot \tau)_\theta + F_\theta \qquad \text{(Eq 4)}$$

Equations 2 to 4 represent a balance between transient and convective fluxes on the left and pressure gradients, diffusion, and source (body force) terms on the right. In these equations, $p$ is static pressure; $\mathbf{U}$ is the generalized velocity vector; $\tau$ is the shear stress tensor; $F = (F_r, F_\theta, F_z)$ is the electromagnetic body force; $r$, $\theta$, and $z$ represent the radial, azimuthal, and axial coordinate directions, respectively; and the subscripts refer to components in the corresponding coordinate directions. These and other symbols are defined in the section on nomenclature. The actual expressions for the body forces and the shear stress will be presented next.

### 2.1 *Shear Stress Tensor*

In general, the stress components can be expressed in terms of the slurry viscosity and the shear rates in tensorial notation as (Ref 4, 5):

$$\tau_{ij} = -\mu\left(\frac{\partial U_i}{\partial X_j} + \frac{\partial U_j}{\partial X_i}\right) \qquad \text{(Eq 5)}$$

where subscripts $i$ and $j$ refer to the coordinate directions, and $U$ and $X$ represent generalized velocity and spatial coordinates, respectively.

Two models are employed to express the slurry viscosity, $\mu$, in Eq 5. The first model assumes that the semislurry system obeys a power-law relationship:

$$\mu = -[m|0.5(\Delta:\Delta)^{1/2}|^{n-1}] \qquad \text{(Eq 6)}$$

where $\Delta$ is the rate of deformation tensor, $(\Delta:\Delta)$ represents the dyadic product of $\Delta$, and m and n are empirical constants defined by the expressions:

$$m = \exp(9.783 f_s + 1.4345) \qquad \text{(Eq 7)}$$

$$n = \begin{cases} 0.1055 + 0.41 f_s & f_s < 0.30 \\ -0.308 + 1.78 f_s & 0.30 \le f_s \end{cases} \qquad \text{(Eq 8)}$$

where $f_s$ is the solid fraction.

It should be pointed out that these relationships are derivatives of those deduced for a lead-tin system by Joly (Ref 2). It is not immediately obvious whether the relationships will hold for the aluminum-copper system considered in the present study. However, it is felt that the general nature of these systems, particularly the shear-thinning behavior, would be fairly well represented by them.

The second alternative constitutive relationship employed is based on the model of Brown (Ref 8), in which the slurry viscosity is obtained from the relationship:

$$\frac{\mu}{\mu_1} = A\left(\frac{(C/C_{max})^{1/3}}{1 - (C/C_{max})^{1/3}}\right) + D f_s \gamma^{(1-n)/n} S \qquad \text{(Eq 9)}$$

where $\gamma = (\Delta:\Delta)^{1/2}$; A, $C_{max}$, and D are empirical constants; and $\mu_1$ is the pure alloy molecular viscosity. The first term on the right is used to express the contribution of relative particle motion to the slurry viscosity and is based on the relationships established by Frankel and Acrivos (Ref 9) for concentrated suspensions of solid spheres. Based on their work, values of A = 9/8 and $C_{max} = 0.625$ were established. C, the effective solid volume fraction, is calculated from:

$$C = f_s(1 + 0.25S) \qquad \text{(Eq 10)}$$

The second term on the right of Eq 9 was derived by Brown to represent the contribution of the disruption of pair bonds (or

degree of agglomeration) in the slurry. This second term is thus used to introduce the time-dependent effect. The degree of agglomeration, $S$, is calculated from:

$$\frac{dS}{dt} = K(1 - S) - GS^2\gamma \quad \text{(Eq 11)}$$

where the first term is called a static hardening function and the second is called a dynamic softening function. K and G (like n in Eq 9) are material constants that, strictly, are dependent on many parameters, including temperature, particle size, solid fraction, shear rate, and fluid properties. The values employed for the constants here are n = 5, K = 0.1, D = $2.5 \times 10^4$, and G = 0.01. These values have been chosen to give steady-state values of viscosity that are close to the Joly-Fleming model.

### 2.2 *Electromagnetic Force*

The electromagnetic force components ($F_r$, $F_\theta$, and $F_z$) in Eq 2 to 4 are evaluated through the Maxwell relations. In the present system, it is assumed that the applied rotating magnetic field is sinusoidal in time and angular coordinates. The force components for a single-pole magnet employed here are approximately (Ref 6):

$$F_z = 0 \quad \text{(Eq 12)}$$

$$F_r = \frac{1}{8} B^2 \left(\bar{\omega} - \frac{w}{r}\right)^2 \sigma\mu_0 r^3 \quad \text{(Eq 13)}$$

$$F_\theta = \frac{1}{2} B^2 \left(\bar{\omega} - \frac{w}{r}\right) \sigma r \quad \text{(Eq 14)}$$

where $\omega$ is the angular velocity of the field, $B$ is its magnitude, $\sigma$ is electrical conductivity, and $\mu_0$ is magnetic permeability.

### 2.3 *Boundary Conditions and Solution of Equations*

The boundary conditions employed in the computations are no slip at the walls, symmetry at the centerline, and zero stress at the free surface. The governing equations were cast in finite-domain forms and solved with the PHOENICS code (Ref 10). A spatially nonuniform 28 by 18 by 36 grid structure was used in the radial, azimuthal, and axial directions, respectively. A fully implicit scheme that is unconditionally stable was employed. The results were found to be grid independent in both the spatial and temporal coordinates.

## 3. Results

Figures 2 and 3 show the velocity vectors at the midheight plane ($z/H = 0.5$). Figure 2 depicts the behavior of the system with a field strength of 0.125 T (tesla) with no solid suspension, and Fig. 3 shows the behavior of a similar system with a solid fraction of 0.4. The system of Fig. 2 was turbulent and Newtonian, and the results were obtained using a turbulence model. It is seen that whereas the maximum velocity is very close to the wall (where the maximum field is located) for the Newtonian flow (Fig. 2), it is located at some distance away for the non-Newtonian case (Fig. 3). The latter behavior is due to the nature of the constitutive relationship. The local shear rate will be at its maximum at some position near the solid surface, which in turn will cause a local minimum in the apparent vis-

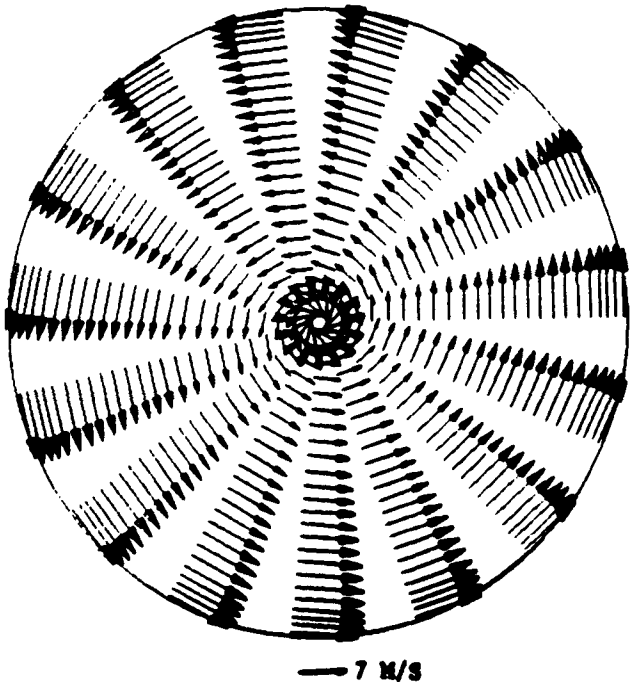


**Fig. 2** Velocity vectors at $z/H = 0.5$ for $f_s = 0$ and $B = 0.125$ T

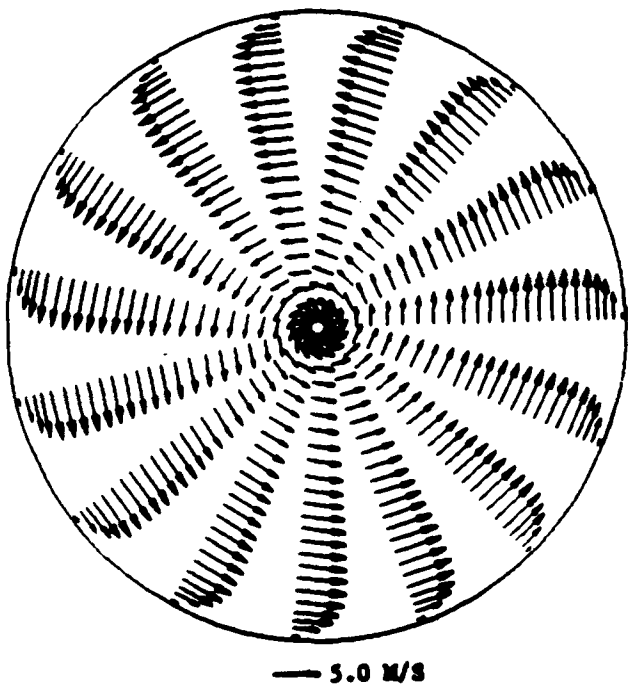


**Fig. 3** Velocity vectors at $z/H = 0.5$ for $f_s = 0.4$ and $B = 0.125$ T

cosity. The net result is a sharper local maximum in the melt velocity than would be expected for turbulent flow conditions.

Figures 4(a) and (b) show maps of solid fraction at different times, in both the absence and presence of stirring, for a system with heat removal at the bottom and heat loss by radiation at the surface. In the absence of agitation, the solid fraction contours are essentially flat, whereas in the presence of agitation, the contours have radial variation. A more detailed description of the solidification model and calculations is given in Ref 6.

Figure 5 shows the evolution of the maximum velocity for a particular case of a solid fraction of 0.3 and a field strength of 0.05 T. The time dependence of the system is readily seen; quasi-steady-state conditions are attained after about 7 s. Figure 6 shows the decay of the characteristic velocity, once the stirring has been discontinued, for the same case. The velocity decays rapidly over a relatively short time. The decay time, of course, will depend on the level of prior agitation.

Figure 7 compares the ratio of maximum value of apparent viscosity to atomic viscosity of the melt computed on the basis of the Brown model (model 1) and the previously published Joly and Flemings model (model 2). It is interesting to note that while the two models differ at the lower shear rates (corresponding to the lower applied field levels), both models tend to converge to quite low values for high levels of agitation. Figure 8 depicts a similar situation, but in terms of the characteristic melt velocity. The two plots are again seen to be quite similar. This indicates that the early model of Joly and Flemings provides a good general representation of the fact that at high shear rates the melt will become quite fluid.

An important aspect of the new modeling approach is that it provides the means for estimating the rate and state of agglomeration within the system. Thus, some of the key issues of inhomogeneity can be addressed. The computed results provide information on the state of agglomeration, which, as seen in Fig. 9 to 12, can be presented either in plots of the field values of $S$ or the maximum values of $S$ as a function of the solid fraction and the applied magnetic field. While the state of agglomeration will vary significantly during the initial stages, it will

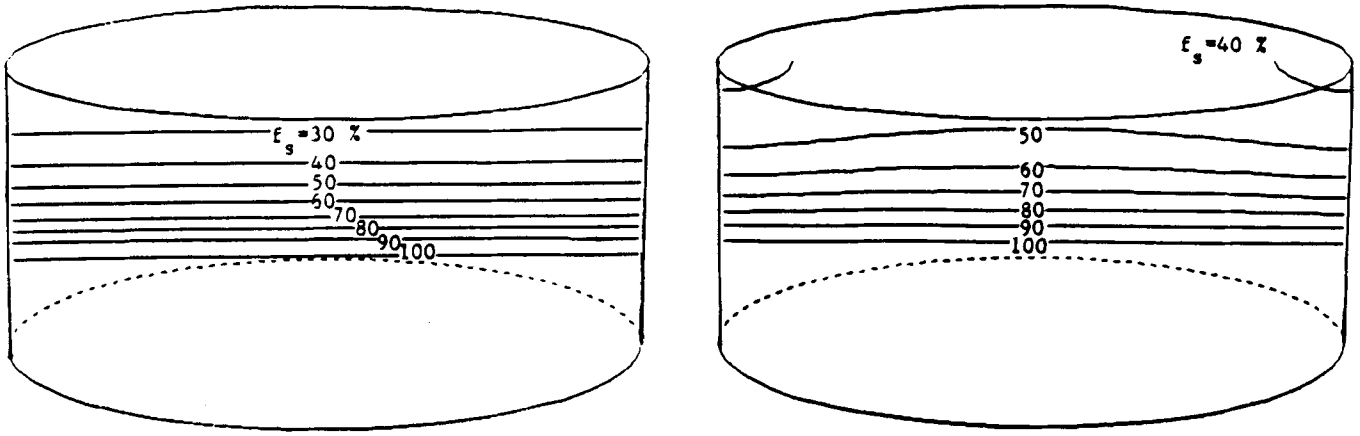


**Fig. 4** Maps of solid fraction after 80 s. (a) $B = 0$ T. (b) $B = 0.125$ T

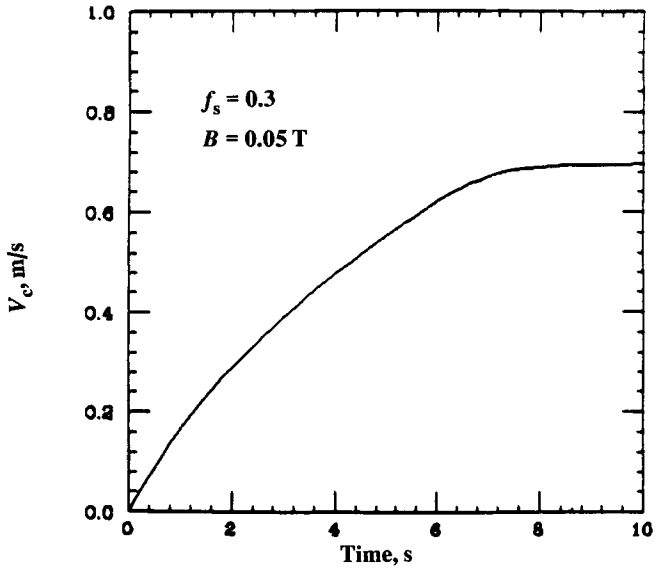


**Fig. 5** Evolution of characteristic velocity

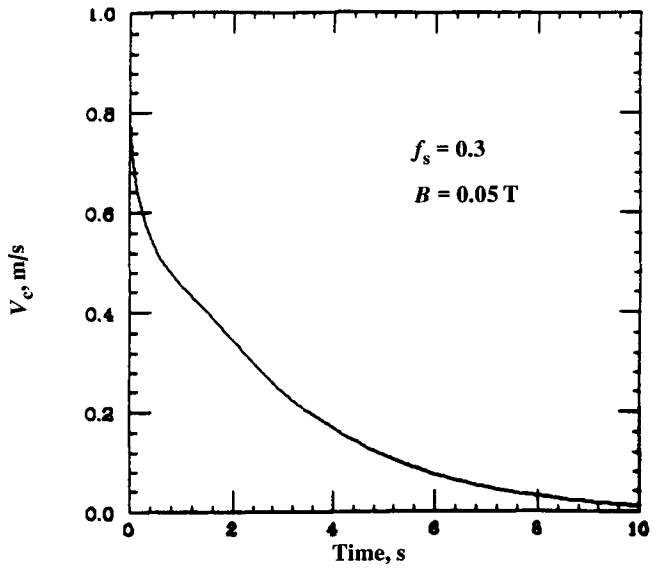


**Fig. 6** Decay of characteristic velocity

become quite uniform after the passage of a certain time period, which was about 8 s in the present case.

## 4. Discussion

A mathematical representation has been developed to describe the velocity fields in an electromagnetically stirred melt/solid slurry consisting of Al-5Cu + $B_4C$. The formulation was based on the Navier-Stokes equations, written for a non-Newtonian fluid exhibiting shear-thinning behavior that can be represented by a power-law-type relationship. Under these conditions, the apparent viscosity will depend both on the shear and on the solid fraction in the melt.

An important feature of this work was to incorporate the time dependence of this relationship. In a physical sense, this time dependence is brought about by the agglomeration of the solid particles. Thus, a finite time must elapse before the system can adjust to a change in the externally imposed conditions, such as the stirring rate. The allowance for time dependence is, of course, a very important practical problem, because time-dependent situations will arise in mold filling and also in the continuous casting of melt/solid slurry systems.

In presenting the computed results, it was possible to compare the predictions based on the Brown model with an earlier model of Joly and Flemings; the latter addressed only the steady-state behavior of the system. With regard to steady-state behavior, the two models were reasonably close at high shear rates and exhibited a behavior where the system became quite

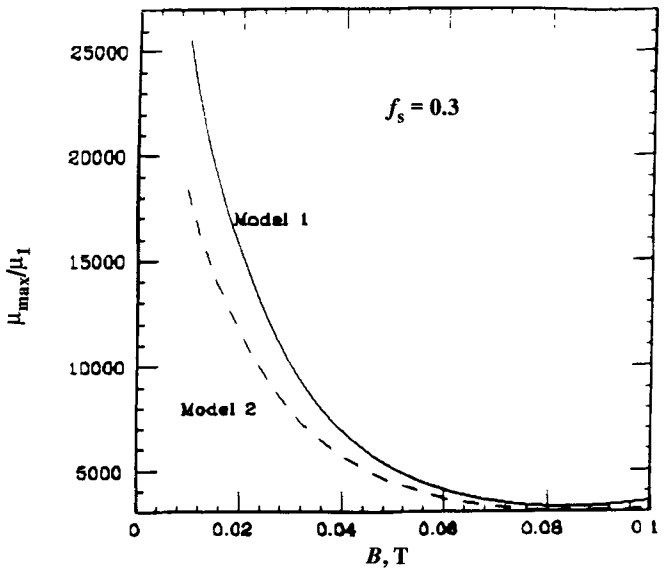


**Fig. 7** Variation of maximum viscosity ratio with magnetic field

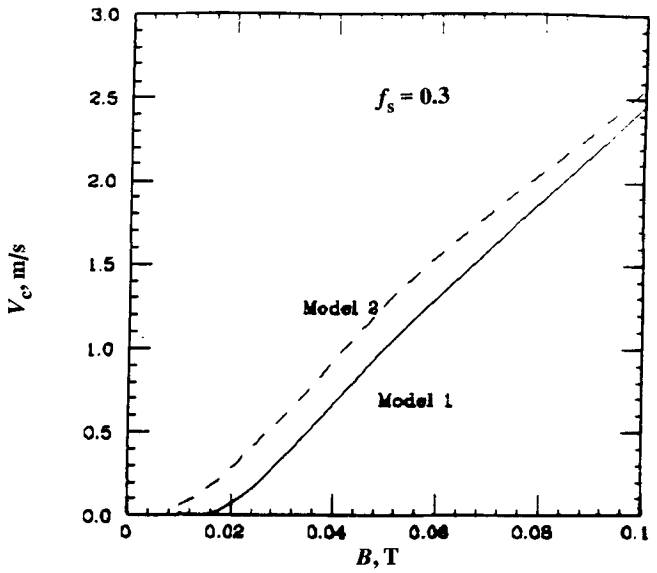


**Fig. 8** Variation of characteristic velocity with magnetic field

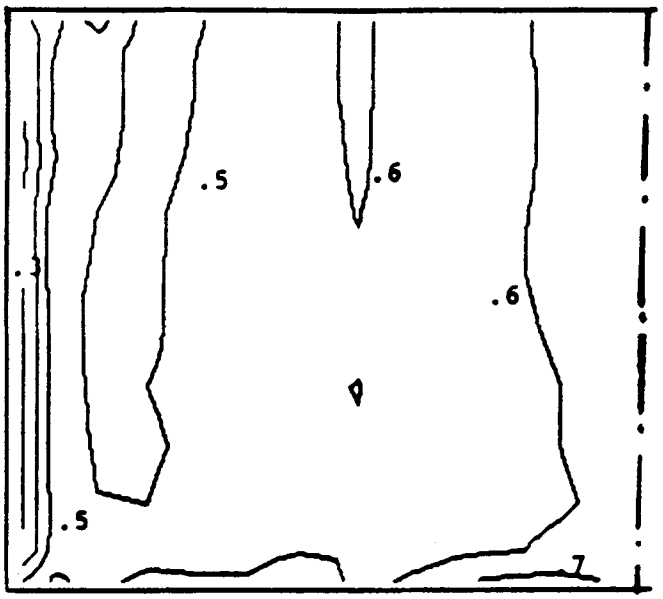


**Fig. 9** Map of $S$ after 1 s ($f_s = 0.3$)

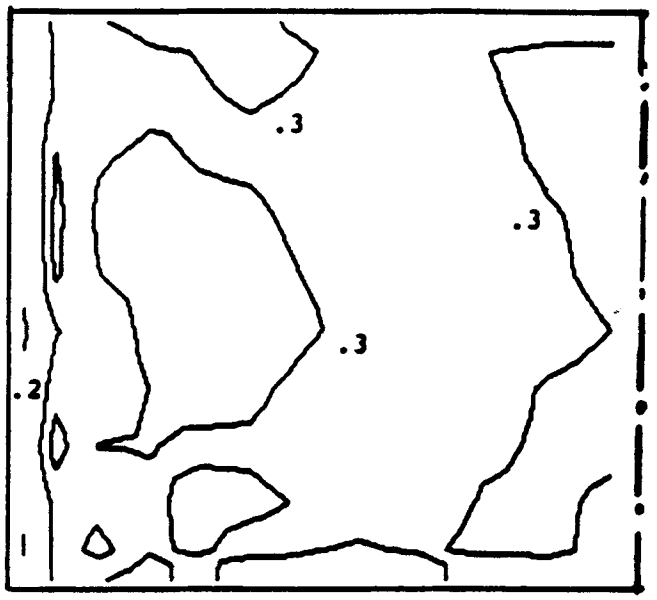


**Fig. 10** Map of $S$ after 10 s ($f_s = 0.3$)

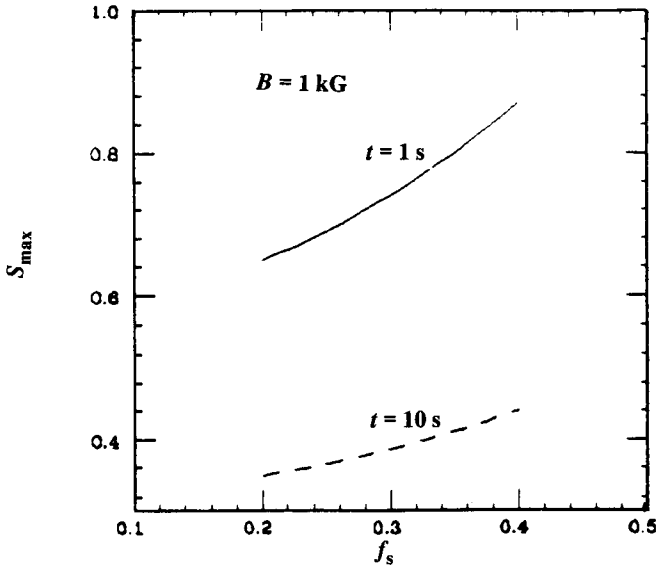


**Fig. 11** Variation of maximum $S$ with solid fraction

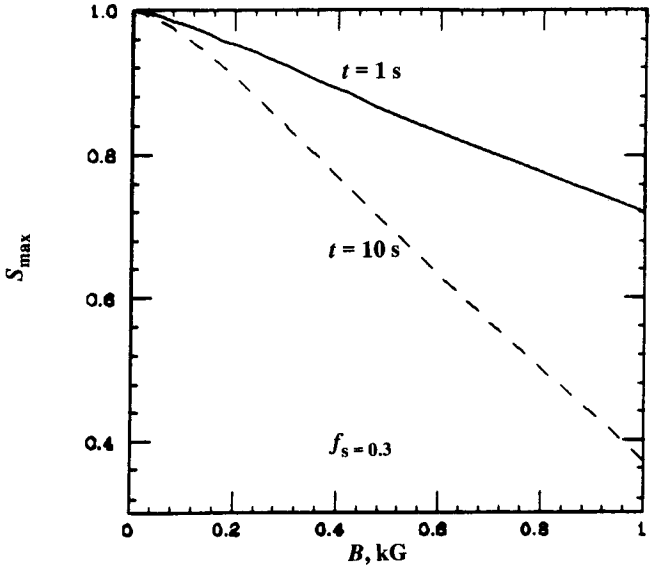


**Fig. 12** Variation of maximum $S$ with magnetic field

fluid once a high enough shear rate was being imposed. Unfortunately, no corresponding experimental data were available for comparison with the predictions for the specific material system considered. However, the mathematical model has been thoroughly compared with analytical and experimental data for other related systems (Ref 4-6). It should also be emphasized that the model of Joly and Flemings with which the present constitutive behavior is compared is based on experimental observation.

An important feature of the model was its ability to predict the transient response of the system to changes in stirring conditions. It was found that for the range of conditions chosen, this response time was on the order of a few seconds, the specifics depending on the solid fraction and on the stirring rate. The important implication of these findings is that rheocast materials can be used to fill molds, but the initial stage of agitation must be quite high and the time span for the actual mold filling application is quite limited.

## Acknowledgments

The author would like to thank Professor Stuart Brown, formerly of the Department of Materials Science and Engineering at MIT, and his students, Pratyush Kumar and Christophe Martin, for useful discussions and suggestions of approximate values for the model constants.

**Nomenclature**

| | |
|---|---|
| A | scaling factor based on assumed spatial particle arrangement |
| $B$ | magnetic field |
| C, $C_{max}$ | effective and maximum volume fraction solid, respectively |
| D | empirical constant |
| $f_s$ | solid fraction |
| $F$ | electromagnetic force |
| G | dynamic softening constant |
| $H$ | height of melt in container |
| K | proportionality constant |
| m, n | empirical constants in shear-stress relationship |
| $p$ | pressure |
| $r$ | radial coordinate |
| $S$ | degree of agglomeration |
| $u$ | velocity component along azimuthal direction |
| U | generalized velocity vector |
| $v$ | velocity component along radial direction |
| $w$ | velocity component along axial direction |
| $z$ | axial coordinate |
| $\Delta$ | rate of deformation tensor |
| $\mu$ | viscosity of slurry |
| $\mu_1$ | viscosity of melt |
| $\mu_0$ | magnetic permeability |
| $\omega$ | angular velocity of magnetic field |
| $\rho$ | density |
| $\sigma$ | electrical conductivity |
| $\tau$ | shear stress tensor |
| $\theta$ | azimuthal coordinate |

## References

1. M.C. Flemings and R. Mehrabian, *Trans. Am. Found. Soc. B,* Vol 17B, 1973, p 119
2. P.A. Joly, Ph.D. thesis, Department of Materials Science and Engineering, Massachusetts Institute of Technology, 1974
3. V. Laxmanan, Ph.D. thesis, Department of Materials Science and Engineering, Massachusetts Institute of Technology, 1979
4. O.J. Ilegbusi and J. Szekely, *Trans. Iron Steel Inst. Jpn.,* Vol 28, 1988, p 97
5. O.J. Ilegbusi and J. Szekely, *Metall. Trans. B,* Vol 21B, 1990, p 183

6. O.J. Ilegbusi and J. Szekely, *Iron Steel Inst. Jpn. Int.*, Vol 29 (No. 6), 1989, p 462
7. O.J. Ilegbusi and J. Szekely, *Iron Steel Inst. Jpn. Int.*, Vol 30 (No. 5), 1990, p 372
8. S. Brown, An Internal Variable Constitutive Model for Semi-solid Slurries, *Proc. 5th Int. Conf. Modeling of Casting, Welding and Advanced Solidification Processes* (Davos, Switzerland), 16-21 Sept 1990, TMS, p 31-38
9. N.A. Frankel and A. Acrivos, *Chem. Eng. Sci.*, Vol 22, 1967, p 847
10. D.B. Spalding, *Math. Comput. Simulation*, Vol XII, 1981, p 267